ORIGINAL PAPER

Microwave-assisted synthesis of gum gellan-cl-poly(acrylic-co- methacrylic acid) hydrogel for cationic dyes removal

Sonal Choudhary[1] · **Kashma Sharma**[1] · **Vijay Kumar**[2] · **Jaspreet Kaur Bhatia**[3] · **Shweta Sharma**[1] · **Vishal Sharma**[1]

Abstract

The present work highlights the microwave-assisted synthesis of novel superabsorbent gum gellan cross-linked poly(acrylic-co- methacrylic acid) hydrogel [GG-*cl*-poly(AA-*co*-MAA)] prepared by the simultaneous graft copolymerization using ammonium persulfate as the initiator and *N,N'*-methylene-*bis*-acrylamide as the cross-linker for the removal of cationic dyes [malachite green (MG) and methylene blue (MB)]. The GG and hydrogel were studied by using Fourier-transform infrared spectroscopy, scanning electron microscopy, and X-ray diffraction spectroscopic techniques. Swelling studies were conducted out in various concentrations of initiator, monomer, and cross-linker. The outstanding dye removal efficiency of ~99% for MG and ~95% for MB was found at the initial dye concentration of 50 mg L^{-1} with an adsorbent dose of 500 mg within the time duration of 6 h and 25 °C. The adsorption kinetics data for both MG and MB dyes exhibited the pseudo-first-order kinetics.

✉ Kashma Sharma
  shama2788@gmail.com

✉ Vijay Kumar
  vj.physics@gmail.com

✉ Vishal Sharma
  sharmavishal05@gmail.com

[1] Institute of Forensic Science and Criminology, Panjab University, Chandigarh 160 014, India

[2] Department of Physics, National Institute of Technology Srinagar, Srinagar, Jammu and Kashmir 19006, India

[3] Postgraduate Department of Chemistry, D.A.V College, Jalandhar, Punjab 144008, India

Introduction

Water pollution produced by the release of enormous amounts of colored waste effluents holding synthetic dyes has ended up being one of the principle environmental issues. These highly toxic colored effluents have an antagonistic effect on water ecosystem and the dangers to human well-being as well [1, 2]. However, these dye wastes are sacked into nature with no water treatment. Maximum of the dyes are harmful, cancer-causing, and deadly chemical, even at very little concentrations [3, 4]. Methylene blue (MB), a cationic hazardous dye, is normally known as 3,7-bis (dimethylamino)-phenothiazin-5-ium chloride. It is regarded to be poisonous than those of other anionic dyes because it can simply percolate into the cells by communicating with the negatively charged surface of cell membranes [5, 6]. Inhalation of methylene blue dye causes a small duration of quick or problematic breathing and correspondingly causes nausea, vomiting, plentiful sweating, mental perplexity, and methemoglobinemia [7–9]. Malachite green (MG) is comprehensively used as biocide in the aquaculture industry and is amazingly active against protozoal and contagious diseases [10, 11]. The US Food and Drug Administration approved MG as an essential chemical for cancer-causing, yet at the same time being used in many regions of the globe because of its cost-effectiveness, easy accessibility, and viability [11, 12]. To overcome these issues, a number of methods such as ion exchange, activated carbon adsorption, membrane technology, and coagulation have been used widely [13]. Among all these strategies, adsorption is examined to be a reliable, highly efficient, simply designed, and economical method with ease of operation. Most of the treatments are observed to be ineffective in the removal of dyes as they decolorize dye by devastating the chromophores, leaving the malefic remaining moieties in the waste.

On the other hand, adsorption can expel dye molecules totally when compared with different strategies. Therefore, in the earlier decades, analysts used different adsorbents, such as activated carbon, clay, chitosan, and farming squander for the elimination of dyes from the wastewater [14–16]. The expanding consideration has been paid to grow high limit adsorbents for the subtraction of dyes from wastewater. Shockingly, complex compound structure and poor biodegradability of many dyes make them recalcitrant chemicals and tend to go through traditional wastewater treatment frameworks unaffected. A hydrogel is a polymer gel constructed through a network of cross-linked polymer chains [17, 18].

Hydrogels are three-dimensional networks of polymer chains that absorb a large amount of water and are resistant to dissolution. Hydrogels are extensively used in industrial and environmental applications because of their higher water absorbing capacity, softness, long-life service, and biocompatibility [19–21]. In recent years, various researchers have been reported the elimination of toxic chemicals comprising synthetic dyes from wastes by hydrogel adsorbents [22–24]. A number of natural polysaccharide-based hydrogels such as guar gum, gum ghatti, gum karaya, kappa carrageenan, gum arabic, chitosan, and xanthan gum were investigated as adsorbents for the expulsion of dyes from an aqueous solution [3, 4, 25–30].

Polymeric hydrogels have received extraordinary consideration due to the presence of SO$_3$H, CONH$_2$, COOH, which can easily captivate metal ions and dye molecules from wastewater [31]. Studies demonstrated that negatively charged functional groups on the anionic hydrogels were extremely practical in binding the positively charged cationic dyes and along these lines expelling them from aqueous solutions [32–34]. Therefore, an anionic hydrogel with greater adsorption ability is an encouraging option for the adsorption of cationic dyes from industrialized wastes.

The goal of this work is to synthesize an anionic superabsorbent hydrogel, GG-*cl*-poly(AA-*co*-MAA) comprising of a natural polysaccharide, and synthetic polymers to be studied as an adsorbent for dyes. This has been attained by polymerizing acrylic acid (AA), methacrylic acid (MAA), and *N,N′*-methylene-*bis*-acrylamide (MBA) in the presence of GG in water, and its effectiveness as an adsorbent for the expulsion of dyes has been carried out using MG and MB as model ionic dyes.

Experimental section

Materials and methods

Gellan gum (GG) was procured from CDH, India. Acrylic acid (AA) and methacrylic acid (MAA), and *N,N*-methylene-bis-acrylamide (MBA) were obtained from Sisco Research Laboratories (India). Ammonium peroxodisulphate (APS) was purchased from Sigma-Aldrich. Malachite green and methylene blue were obtained from Sisco Research Laboratories (India). All other reagents were used as received. Deionized water was used during the course of the synthesis processes.

Preparation of GG-*cl*-poly(AA-*co*-MAA)-*based hydrogels*

A polymer framework made out of GG-*cl*-poly(AA-*co*-MAA) was synthesized by utilizing an MBA as cross-linker and APS as initiator under microwave irradiation. In this investigation, 0.5 g gum gellan was broken down in 10 ml of deionized water in a reaction flask. The complete synthesis procedure was reported in our previous work [26]. The percentage swelling (P_s) and percentage grafting (P_g) were also computed by using the procedure reported earlier [26]. The percentage grafting and swelling were calculated using the following equations:

$$P_g = \frac{W_f - W_b}{W_b} \times 100 \tag{1}$$

$$P_s = \frac{W_s - W_d}{W_d} \times 100 \tag{2}$$

where, W_f, W_b, W_s, and W_d are the weight of the functionalized polymer backbone, swelled and dry samples, respectively.

Characterization

Microwave oven IFB model-17PM-MEC1 of power source: 230 V ~ 50 Hz, power consumption: 1200 W with a frequency of 2450 MHz is utilized for illumination. The FTIR spectra were recorded using FTIR spectrometer (PerkinElmer) furnished with ATR mode having diamond crystal and ZnSe for focusing part. The parameters of the scan with a resolution of 4 cm^{-1} in the range of 4000–400 cm^{-1} were taken. Adsorption investigations of malachite green on the cross-linked hydrogels were done utilizing Shimadzu UV-Vis spectrophotometer at room temperature. Absorption spectra were taken in the range of 400–700 nm. X-ray studies were completed on the X'Pert Pro model and make PANanalytical, Netherlands diffractometer. The diffraction pattern was recorded at an angle in the range of 10°–70° at a scan speed of 2° min^{-1}. Morphological investigation of samples was obtained using Joel (Japan) scanning electron microscope, JSM 6100 model.

Adsorption studies

A known quantity of GG-cl-poly(AA-co-MAA) hydrogel was left dipped in 50 mg/L solutions of MG and MB dyes. At time intervals of 20 min, 2.5 mL of the filtered solution was reserved and the absorbance values were noted by employing UV–visible spectrophotometer for MG and MB. Standardization curves were employed to convert the absorbance measured into concentration using standard solutions of 2, 4, 6, 8, and 10 mg/L of the dyes. Diverse initial concentrations (10, 20, 30, 40, 50, and 60 mg/L) were used for equilibrium adsorption studies by dipping varied quantity of the sample and kept for 6 h, and the later solutions were transferred, and the absorbance was noted down. The amount of solute uptake with time and is given in Eq. (3) [35].

$$\frac{dq_t}{dt} = k_1(q_e - q_t) \tag{3}$$

On integrating Eq. (3) within the limits $q_t = 0$ at $t = 0$ to $q_t = q_e$ at $t = t$ and converting it into linear form, the equation becomes

$$\log(q_e - q_t) = \log q_e - \frac{k_1}{2.303}t \tag{4}$$

where q_e and q_t are the adsorption capacity at equilibrium and at time t (min), respectively. k_1 is rate constant of pseudo-first-order adsorption (min^{-1}). The values of k_1 and q_e can be calculated from the plot of log $(q_e - q_t)$ versus t for different initial concentrations. Pseudo-second-order equation is expressed as Eq. (5) as:

$$\frac{dq_t}{dt} = k_1(q_e - q_t)^2 \tag{5}$$

On integrating equation within the limits and converting into linear form, Eq. (6) is obtained

$$\frac{t}{q_t} = \frac{1}{k_2 q_e^2} + \frac{1}{q_e}t \tag{6}$$

where k_2 is pseudo-second-order rate constant (g mg^{-1} min^{-1}). q_e and k_2 values can be calculated from slope and intercept of plots of t/q_t vs t. The experimental results were further fitted to Weber's intraparticle diffusion to make clear the diffusion mechanism. The model is expressed as Eq. (7).

$$q_t = k_i t^{1/2} + C \qquad (7)$$

where q_t is the amount of dye adsorbed on the surface of adsorbent at time t. k_i is intraparticle diffusion rate constant (mg/g min$^{1/2}$). The kinetic models were further validated for their applicability by normalized standard deviation Δq (%) which is given in Eq. (8).

$$\Delta q\,(\%) = 100 \times \sum \frac{[(q_{exp} - q_{cal})/q_{exp}]^2}{N - 1} \qquad (8)$$

where N is the number of data points, q_{exp} and q_{cal} (mg/g) are the experimental and calculated adsorption capacity, respectively.

Results and discussion

Influence of various parameters on percentage of swelling (P_s)

The percentage of swelling (P_s) of the GG-cl-poly(AA-co-MAA) hydrogel in different initiator concentration (APS) (0.0087 mol/L to 0.02629 mol/L) were studied and the results reported in Fig. 1a. The P_s was observed to be expanded at first varying the initiator content up to 0.01753 mol/L after that its water engrossing capacity diminished because of free radical degradation of the backbone (Fig. 1a). Maximum percentage swelling (217%) was figured at 0.01753 mol/L of initiator concentration [26]. The swelling capacity was likewise affected by the solvent concentration. Figure 1b demonstrates that P_s first improved up to 6 mL of solvent (292%) and after that diminished because of the way that at an ideal amount of solvent there is a generation of hydroxyl radical ions giving more active sites for the propagation of reaction prompts to increasing P_s. The solvent concentration is increased from its optimized amount P_s began decreasing on the grounds that there are lesser active sites for graft polymerization over gum gellan backbone and on monomers [36].

The monomer concentration plays a significant part in the swelling capacity of the hydrogels. For optimization, binary-monomers concentration (AA-MAA) was varied in ratio from 0.03603 mol/L: 0.08609 mol/L to 0.07206 mol/L: 0.08609 mol/L to get maximum P_s value (292%) (Fig. 1c). After that, further increase in bi-monomer concentration hinders the swelling capacity as shown in the figure because of AA-MAA monomer cause oversaturation [26]. The cross-linker makes hydrogel insoluble in water by inhibiting the termination of hydrophilic polymer chains in an aqueous solution. The optimized value of cross-linker is 0.054 mol/L for grafted copolymer exhibiting a maximum swelling capacity of 292% (Fig. 1d). Beyond this, P_s decreased due to the formation of a compact and rigid structure [37]. The optimized parameters are given in Table 1.
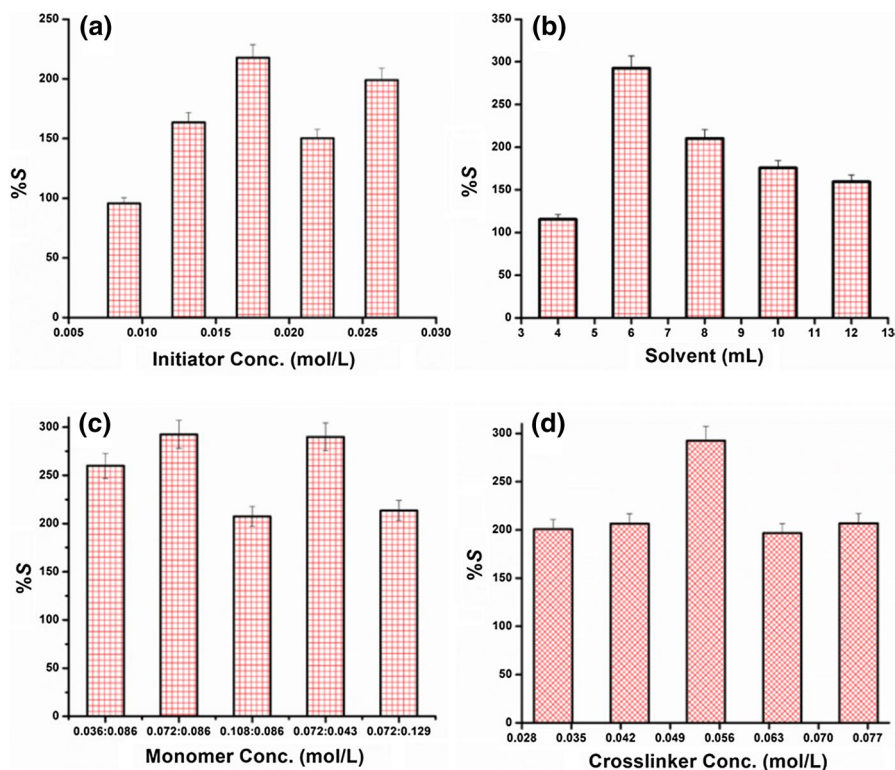
Fig. 1 Variation of P_s with **a** initiator concentration, **b** amount of solvent, **c** monomer concentration, and **d** cross-linker concentration
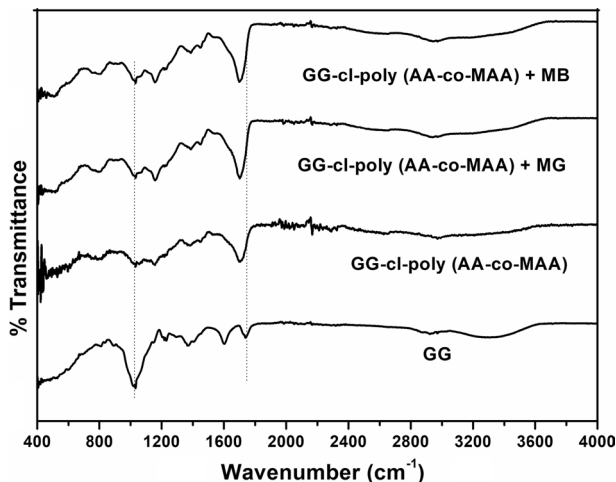
FTIR spectral analysis of hydrogels

FTIR spectra of GG, GG-cl-poly(AA-co-MAA) hydrogel, GG-cl-poly(AA-co-MAA)-MG-loaded hydrogel, and GG-cl-poly(AA-co-MAA)-MB-loaded hydrogel are shown in Fig. 2. The spectrum of GG shows a wide peak at 3294 cm$^{-1,}$ 1739 cm^{-1}, 1603 cm$^{-1,}$ 1369 cm^{-1}, 1226 cm^{-1}, and 1026 cm^{-1} corresponds to hydroxyl absorbance (–OH), acid carbonyl –C=O stretching bond, C=C stretching vibrations [38], ionization of COO$^-$ and –C=O, and stretching and bending vibrations of N–H [39]. After the cross-linking of binary monomers over the surface of gum gellan, new peaks were observed with a varying intensity which confirms the successful grafting of gum gellan with acrylic acid and methacrylic acid. GG-cl-poly(AA-co-MAA) hydrogel shows –C–H bond on the saturated carbon atom at 2973 cm^{-1} [40]. The peaks at 1705 cm^{-1} are credited to –C=O stretching vibrations of the carboxylic group [41], and the peaks at 1452 cm^{-1}, 1385 cm^{-1} are due to the absorption of –OH bending vibrations from –COOH and C–N stretching vibrations [42]. The band at 1159 cm^{-1} indicates –C–O stretching vibrations [39]. There are also other peaks observed when methylene blue and

Table 1 Optimized reaction parameters for the synthesis of GG-cl-poly(AA-co-MAA)

Backbone (g)	Initiator conc. [mol $L^{-1} \times 10^{-2}$]	Solvent [mL]	Monomer conc. [mol $L^{-1} \times 10^{-2}$]	Cross-linker conc. [mol $L^{-1} \times 10^{-2}$]	Time [sec]	Temp. [°C]	Mean P_g	Mean P_s	±SD	±SE
0.5	1.753	6	7.206:8.609	5.405	60	60	165	292	35.7	20.6

±SD Standard deviation, ±SE Standard error, P_s Percentage swelling

Fig. 2 FTIR spectra of GG, GG-cl-poly(AA-co-MAA) hydrogel, GG-cl-poly(AA-co-MAA)-MG-loaded hydrogel, and GG-cl-poly(AA-co-MAA)-MB-loaded hydrogel

malachite green dyes are adsorbed over the cross-linked network of hydrogel at 2939 cm^{-1}, 2943 cm^{-1}, 1709 cm^{-1} which is due to the symmetric stretching, scissoring, and rocking vibrations of a methylene group, –CH stretching vibrations, and –C=O stretching of acids [43]. Peak band at 1456 cm-1, 1388 cm^{-1} shows absorption of –OH bending vibrations from COOH and C-N stretching vibrations [42] and the bands at 1162 cm^{-1} credited to –C=O stretching vibrations [44]. 1030 cm^{-1} is ascribed to –C–O–C– stretching vibrations [43].

XRD

The X-ray diffractograms of GG, GG-cl-poly(AA-co-MAA) hydrogel, GG-cl-poly(AA-co-MAA)-MG-loaded hydrogel, and GG-cl-poly(AA-co-MAA)-MB-loaded hydrogel are compared as displayed in Fig. 3. The GG shows a diffraction peak at an angle of 20.0 in 2θ scale. This indicates that GG is semi-crystalline with dominant amorphous character. After the formation of GG-cl-poly(AA-co-MAA) hydrogel, then it becomes more crystalline as a sharp peak is observed and shifts toward the lower angle (17.7°). The shifting of the modified gum peak indicates that grafting of binary monomers over the smooth surface of gum gellan makes it crystalline. This confirms the successful cross-linking of AA and MAA over the gum gellan. The gum gellan shows percentage crystallinity of 38.0. But during the formation of GG-cl-poly(AA-co-MAA) hydrogel, the percentage crystallinity increases up to 49.5, indicating that the amorphous form of the gum is lost which is easily predicted from the graph. There is a large increase in the percentage crystallinity of GG-cl-poly(AA-co-MAA)-MG-loaded hydrogel and GG-cl-poly(AA-co-MAA)-MB-loaded hydrogel, i.e., 55.0 and 53.8. The grafted hydrogel GG-cl-poly(AA-co-MAA) with adsorbed dyes shows more shift of peak toward lower 2θ angle over the two peaks of GG and GG-cl-poly(AA-co-MAA) hydrogel with an angle of 17.6 and
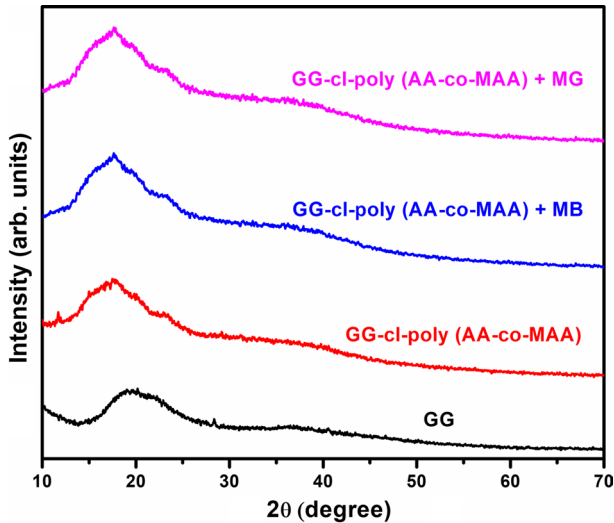
Fig. 3 X-ray pattern for GG, GG-cl-poly(AA-co-MAA) hydrogel, GG-cl-poly(AA-co-MAA)-MG-loaded hydrogel, and GG-cl-poly(AA-co-MAA)-MB-loaded hydrogel

17.5 in 2θ scale. This concludes that after the adsorption of the dyes on the cross-linked hydrogel, there is an increase in crystallinity as shown in figure peak becomes sharper [26].

Scanning electron microscopy of hydrogels

The surface morphology of GG and GG-cl-poly(AA-co-MAA) hydrogel is displayed in Fig. 4. There is an ample difference in their morphology as GG has a globular-like structure with a smooth and roughed surface. After cross-linking with poly(AA-MAA), GG-cl-poly(AA-co-MAA) hydrogel structural morphology got changed, the structure becomes spikes like due to the network formation confirms the grafting of poly(AA-MAA) on the surface [26, 45].

Dye removal studies

The synthesized hydrogel has anionic nature that may help the cationic dye diffused within the interior network resulting in the removal of dye from wastewater. The hydrogel was prepared by using hydrophilic binary monomers under microwave irradiation that increases the void size in the polymer matrix and give more surface area for adsorption. To investigate the dye adsorption capacity, 100 mg–600 mg of hydrogel samples were taken for investigation. Malachite green and methylene blue were used as model cationic dyes. The graphical representation of adsorbed malachite green dye is shown in Scheme 1. The result of dye concentration, adsorbent
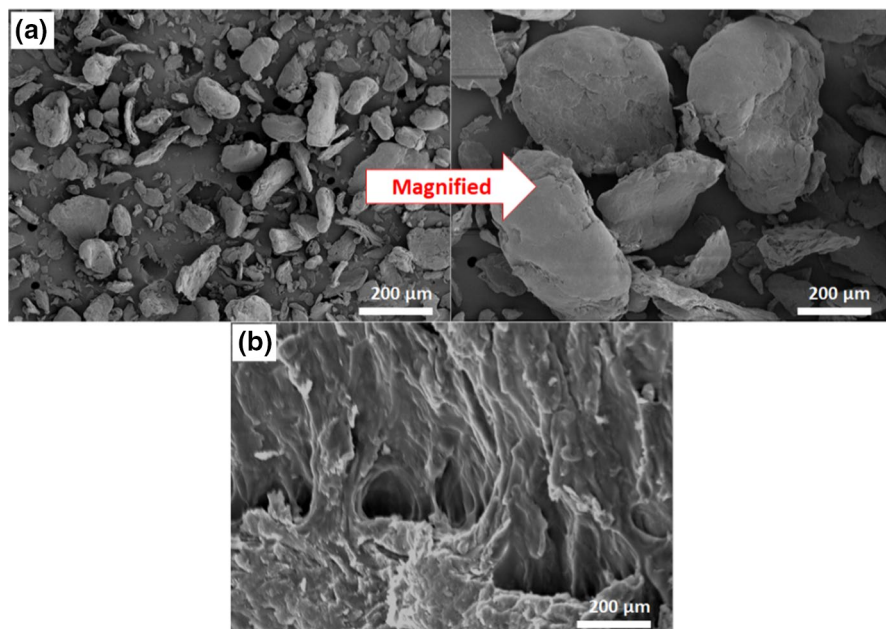
**Fig. 4** SEM micrographs of **a** gellan gum, and **b** GG-cl-poly(AA-co-MAA)

concentration, and influence of pH on dye removal efficiency was described in the next paragraphs (Fig. 5).

Effect of adsorbent concentration

A promising adsorbent material is required to get rid of goodly extents of dyes at a very low amount. This part is very important to cut back functioning prices and lessen the hazards associated with secondary contamination [46]. The increment in the adsorbent dose initially improved the dye removal capacity. By and large, the expansion of the amount of hydrogel up to 0.5 g enlarged the adsorption sites permitting more dye-hydrogels interactions and enhancing the removal process for both malachite green and methylene blue dyes (Fig. 4a, d) [47, 48]. However, more increase in the adsorbent concentration can decrease the surface adsorption ability as result surface interactions between the adsorbent molecules cause accumulation, thereby dropping the number of accessible surface sites hence damaging the adsorption values [49].

Effect of dye concentration

The adsorption studies were done at ambient temperature by varying the concentration of methylene blue and malachite green while keeping the other parameters fixed (Fig. 4b, e). In both the dyes, increase in the concentration beyond 50 ppm
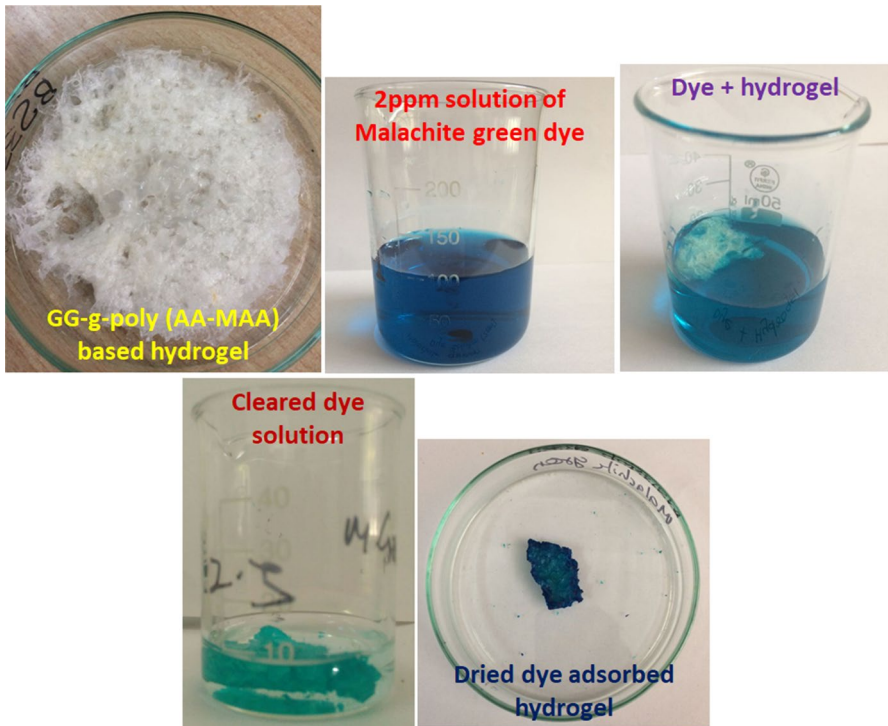
Scheme 1 The pictorial representation of adsorbed malachite green dye

adsorption decreases, and this can be possible because of the saturation of the adsorption sites on the adsorbents [8, 50]. The adsorption was found to be maximum at 50 ppm in both the dyes.

Effect of pH

pH change is a crucial factor influencing the adsorption process by converting functional groups into an ion or ions dispersed along with the hydrogel sites. The functional moieties change the adsorbent–adsorbate balance, its adhesion mechanism, and kinetics [3, 4, 46, 51]. Below acidic conditions, the adsorption of MB dye was reduced because active functional groups of adsorbent were protonated and lessening their contact with the MB and MG dyes molecule (Fig. 4c, f). Also, the H^+ ions accessible in the mixture interact with the MB molecules for the adsorption sites. While in neutral conditions, the adsorbents were negatively charged because of the removal of protons from the –COOH groups leading in increased MB adsorption. Also, negatively charged groups improved the anion–anion repulsive forces resulting in network growth and enhancement in MB removal from the water [52].
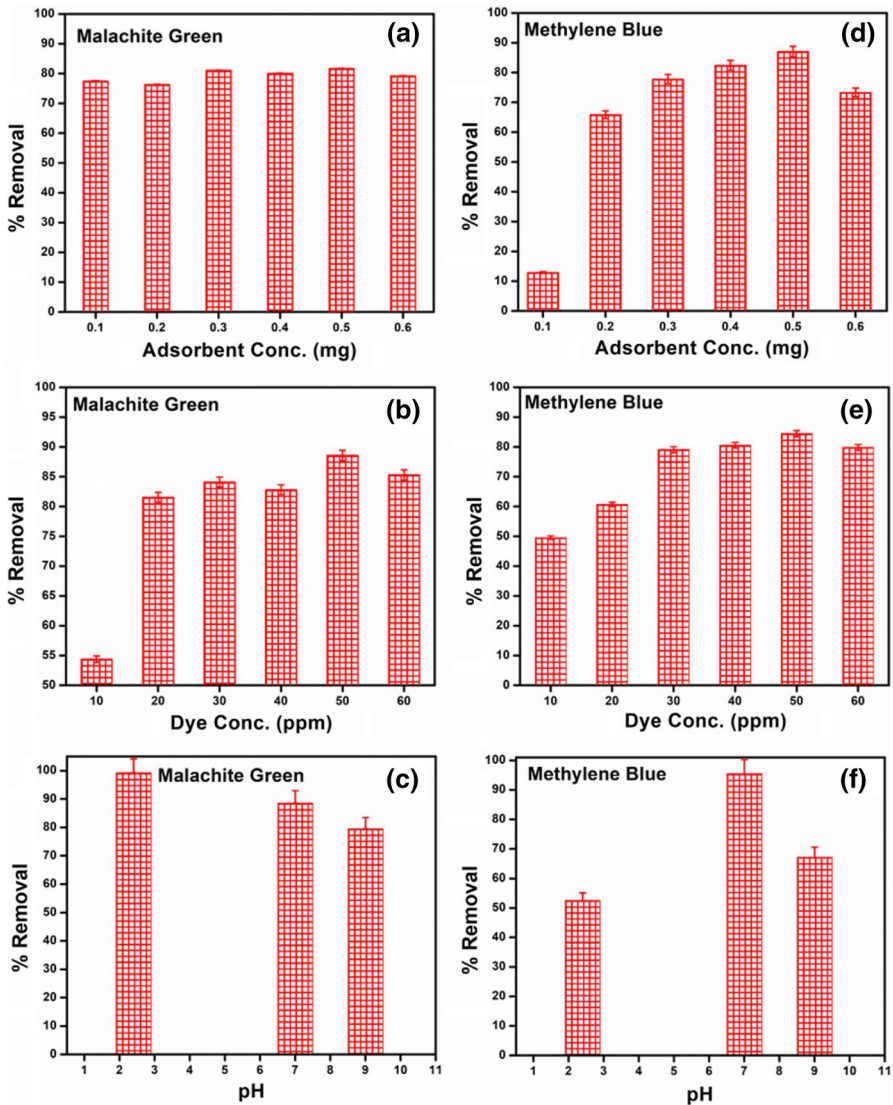
Fig. 5 Effect of adsorbent concentration, dye concentration, and pH for **a–c** malachite green dye and **d–f** methylene blue dye

Malachite green showed the greatest adsorption in acidic pH as compared to basic and neutral pH. This may be due to the fact that there is a strong interaction between the anionic gel and cationic dye. This will enhance its adsorption capacity [45]. As appeared in the figure, the adsorption of MG dye increases under acidic pH owing to the formation of strong electrostatic interactions among

the negatively charged groups of GG-g-poly(AA-MAA) and positively charged groups of MG dye [53].

Plausible mechanism

The polymerization is a free radical process which initiates grafting of poly(AA) and poly(MAA) chains on the gellan gum. A cross-linked system of gum gellan and poly(acrylic-co-methacrylic acid) (GG-*cl*-poly(AA-*co*-MAA) is prepared by the simultaneous graft copolymerization using ammonium persulfate as the initiator
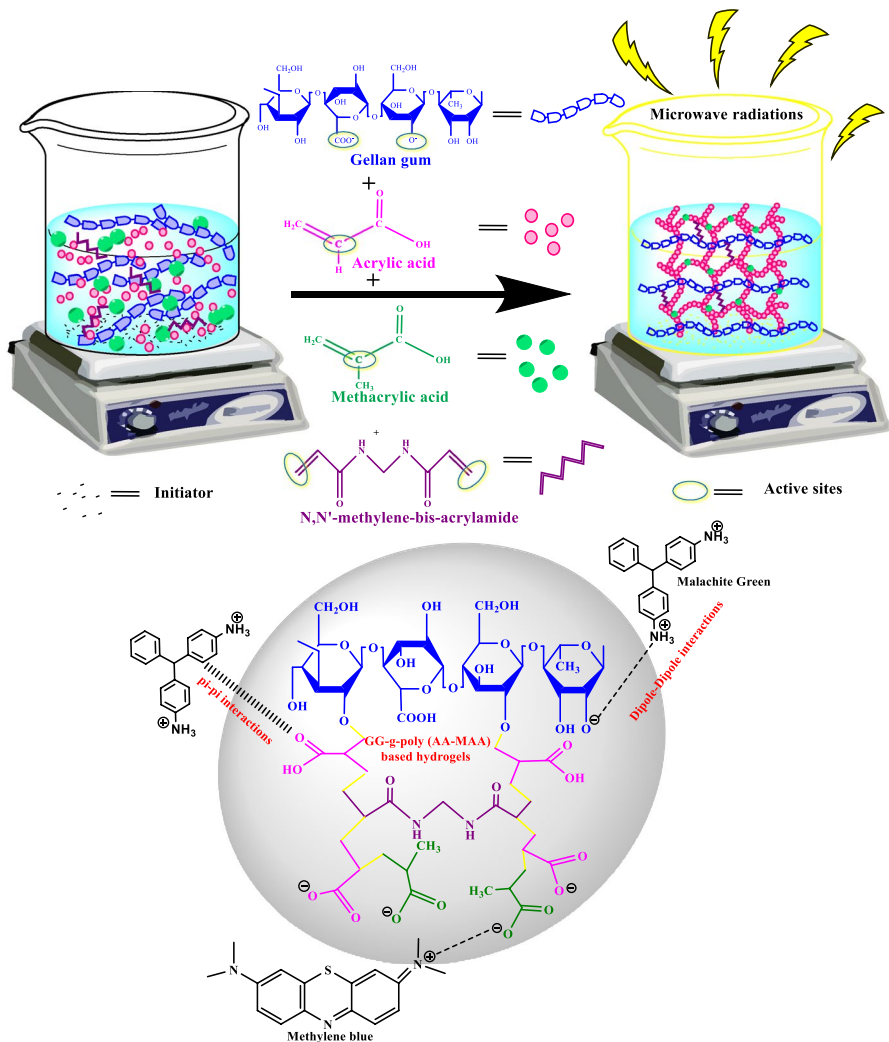

Scheme 2 Schematic representation for the synthesis of GG-cl-poly(AA-co-MAA) and interaction of hydrogel network with MB and MG dye molecules

and *N,N′*-methylene-*bis*-acrylamide as the cross-linker under microwave radiations (Scheme 2). Dye molecules were absorbed into the hydrogel network gradually by interacting through H-bonding, ionic interactions, and van der walls forces [28]. This went on until the saturation level was achieved.

Adsorption kinetics

With the end goal to look at the controlled mechanism of adsorption process, pseudo-first-order, pseudo-second order, and intraparticle diffusion equations are utilized to verify experimental data of both MG and MB dyes (Fig. 6). Lagergren pseudo-first-order equation demonstrates that the rate of change of solute uptake with time is specifically identified with the distinction in the measure of solute uptake at equilibrium and the amount of solute uptake with time as given
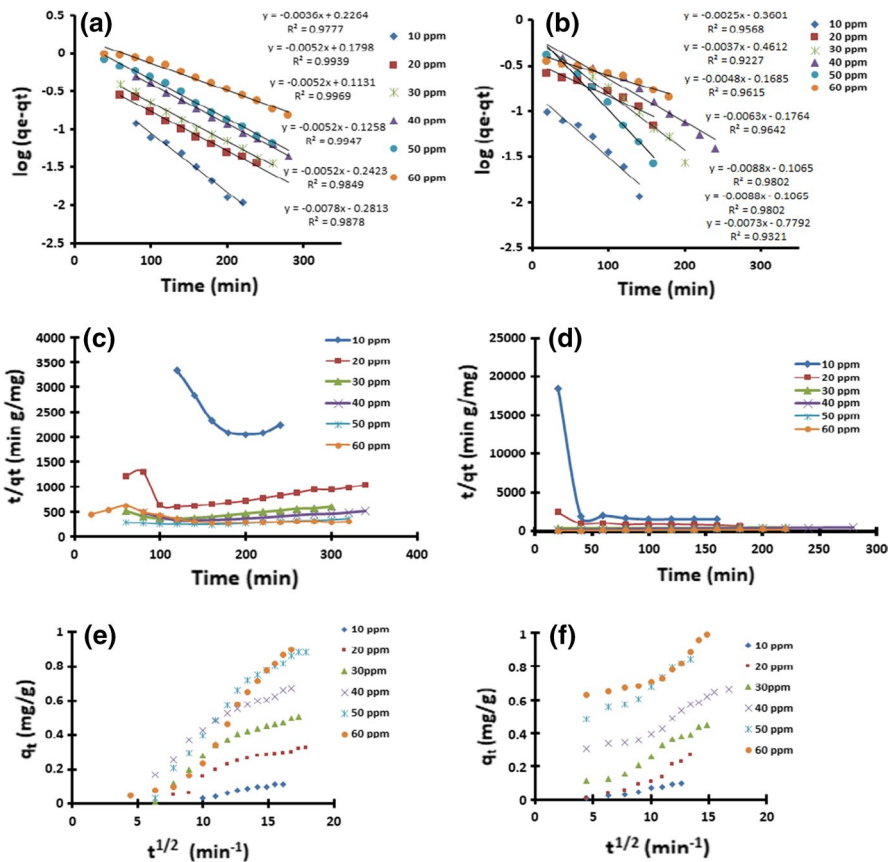
Fig. 6 Pseudo-first-order kinetic model for **a** malachite green dye adsorption **b** methylene blue dye adsorption. Pseudo-second-order kinetic model for **c** malachite green dye adsorption **d** methylene blue dye adsorption. An intraparticle diffusion model for adsorption of **e** malachite green dye **f** methylene blue dye on the adsorbent

by Eq. (3) [35]. The values of k_1 and q_e can be computed from the plot of log $(q_e - q_t)$ versus t for different initial concentrations as shown in Fig. 6a, b.

Parameters of pseudo-first-order and pseudo-second-order for both dyes are given in Table S1 (supplementary data). Comparison of theoretical and experimental values of q_e for the pseudo-first-order and pseudo-second-order kinetics demonstrated that pseudo-first order is more suitable for depicting the sorption system in the event of MG as well as MB dyes. The theoretical values of q_e are nearer to experimental values of q_e for pseudo-first-order kinetic model because q_e values computed by the pseudo-second-order kinetic model show the vast difference from the experimental value. Likewise, linear fitting of pseudo-first-order model gives the better value of correlation coefficient (R^2) than that for the pseudo-second-order kinetic model. The test results were further fitted to Weber's intraparticle diffusion to illustrate the diffusion mechanism (Eq. 7) [54]. Constant C and k_i can be figured from the intercept and slope of q_t versus $t^{1/2}$ plot (Fig. 6c, d). The constant C reveals the boundary layer effect; larger value of the intercept shows a noteworthy impact of surface sorption as a rate controlling step. The linear relationship between q_t and $t^{1/2}$ shows that intraparticle diffusion is engaged in adsorption process, and if the line passes through the origin, it uncovers that intraparticle diffusion is a controlling step, whereas if the line does not pass through the origin, it demonstrates that there is some level of the boundary, but intraparticle diffusion is not the main controlling process and other processes may likewise control the rate of adsorption [55]. The q_t versus $t^{1/2}$ plots (Fig. 6e, f) show multilinear which indicates the presence of two or more step adsorption process. At higher concentrations (40–60 ppm for MG and 30–60 ppm for MB), plots show three portions. The initial curved boundary is due to surface adsorption and fast boundary diffusion. The second linear region is a regular adsorption step where diffusion is the rate controlling step. A third part is the equilibrium stage where intra-particle diffusion slows down due to low solute concentration. While at low concentrations (10–30 ppm for MG and 10–20 ppm for MB), initial curve portion is missing in case of low initial concentration adsorption start gradually having diffusion as a rate controlling process followed by an equilibrium stage. Moreover, the lines do not pass through the origin, which indicates that the diffusion is not the only process involved in adsorption and adsorption is a multistep process in both cases [8].

Validity of kinetic models

The kinetic models were further validated for their applicability by normalized standard deviation Δq (%) calculated by Eq. 8 [56]. The lower value of Δq (%) indicates a better fit of the model. Table S1 shows that Δq (%) values of the first-order kinetic model were in the range of 1.65–8.18% (MG) and 1.29–4.95 (MB), where the second-order model has a much higher value in both cases. This is in concurrence with the R^2 values acquired for the two models and affirms that adsorption of dyes could be best depicted by the pseudo-first-order kinetic model.

Conclusion

In this work, new eco-friendly gum gellan (GG) cross-linked poly(acrylic-co-methacrylic acid) hydrogel [GG-*cl*-poly(AA-*co*-MAA)] hydrogels were prepared by an effective and green technology for the efficient removal of methylene blue (MB) and malachite green (MG). The synthesized GG-cl-poly(AA-co-MAA) hydrogel has been characterized by Fourier-transform infrared spectroscopy (FTIR), scanning electron microscopy (SEM), and X-ray diffraction (XRD) spectroscopic techniques. The synthesized hydrogel candidate shows 165% percentage grafting (P_g) with 292% percentage swelling (P_s) capacity. The good swelling capacity is due to the presence of hydrophilic monomer in the hydrogel. This facilitates GG-cl-poly(AA-co-MAA) hydrogel to be used as a successful device for wastewater treatment. The FTIR investigations indicate variations in the intensity of the peaks and presence of new peaks that show the grafting of poly(AA-MAA) chains over gum gellan. The synthesized GG-cl-poly(AA-co-MAA) hydrogel has been effectively employed for the removal of malachite green dye and methylene blue from water. The dye adsorption studies have been characterized by UV–vis spectrophotometer. The adsorption isotherm model is useful to study the order of the sorption system. The aforementioned study investigated that GG-cl-poly(AA-co-MAA) hydrogel can be regarded as an encouraging superabsorbent hydrogel candidate for the remediation of wastewater treatment. We are probably aware of the fact that dyes are the most widely recognized harmful molecules which pay a noteworthy danger to the living organism, as water toxins. This is essential in decreasing waste material and controlling contamination from industrial areas. The capable synthesis technique and brilliant adsorption properties enable GG-cl-poly(AA-co-MAA) hydrogel to be a better candidate to expel dyes from industrial effluents.

References

1. Daneshvar E, Kousha M, Jokar M, Koutahzadeh N, Guibal E (2012) Acidic dye biosorption onto marine brown macroalgae: isotherms, kinetic and thermodynamic studies. Chem Eng J 204–206:225–234
2. Kang Q (2007) Residual color profiles of simulated reactive dyes wastewater in flocculation processes by poly-diallyldi-methylammoniumchloride. Sep Purif Technol 57:356–365
3. Mittal H, Maity A, Ray SS (2015) Effective removal of cationic dyes from aqueous solution using gum ghatti-based biodegradable hydrogel. Int J Biol Macromol 79:8–20
4. Mittal H, Maity A, Ray SS (2015) Synthesis of co-polymer-grafted gum karaya and silica hybrid organic-inorganic hydrogel nanocomposite for the highly effective removal of methylene blue. Chem Eng J 279:166–179

5. Gomes RF, Neto-de-Azevedo AC, Pereira AGB, Muniz EC, Fajardo AR, Rodrigues FHA (2015) Fast dye removal from water by starch-based nanocomposites. J Colloid Interf Sci 454:200–209

6. Jiao TF, Guo HY, Zhang QR, Peng QM, Tang YF, Yan XH, Li BB (2015) Reduced graphene oxide-based silver nanoparticle-containing composite hydrogel as highly efficient dye catalysts for waste-water treatment. Sci Rep 5:11873–11884

7. Mall ID, Srivastava VC, Agarwal NK, Mishra IM (2005) Removal of congo red from aqueous solution by bagasse fly ash and activated carbon: kinetic study and equilibrium analyses. Chemosphere 61:492–501

8. Mall ID, Srivastava VC, Kumar GVA, Mishra IM (2006) Characterization and utilization of mesoporous fertilizer plant waste carbon for adsorptive removal of dyes from aqueous solution. Colloids Surf A Physicochem Eng Aspects 278:175–187

9. Mall ID, Srivastava VC, Agarwal NK, Mishra IM (2005) Adsorptive removal of malachite green dye from aqueous solution by bagasse fly ash and activated carbon-kinetic study and equilibrium isotherm analyses. Colloids Surf A Physicochem Eng Aspects 264:17–28

10. Hashimoto JC, Paschoal JAR, Ferraz de Queiroz J, Reyes FGR (2011) Considerations on the use of malachite green in aquaculture and analytical aspects of determining the residues in fish: a review. J Aquat Food Product Tech. 20:273–294

11. Schnick RA (1988) The impetus to register new therapeutants for aquaculture. Prog Fish Cult 50:190–196

12. Culp SJ, Beland FA (1996) Malachite green: a toxicological review. J Am Coll Toxicol 15:219–238

13. Ong ST, Lee CK, Zainal Z (2007) Removal of basic and reactive dyes using ethylene-diamine modified rice hull. Bioresour Technol 98:2792–2799

14. Galán J, Rodríguez A, Gómez JM, Allen SJ, Walker GM (2013) Reactive dye adsorption onto a novel mesoporous carbon. Chem Eng J 219:62–68

15. Machado FM, Bergmann CP, Fernandes THM, Lima EC, Royer B, Calvete T, Fagan SB (2011) Adsorption of reactive red M-2BE dye from water solutions by multiwalled carbon nanotubes and activated carbon. J Hazard Mater 192:1122–1131

16. Kyzas GZ, Lazaridis NK, Kostoglou M (2014) Adsorption/desorption of a dye by a chitosan derivative: experiments and phenomenological modeling. Chem Eng J 248:327–336

17. Liu Y, Zheng Y, Wang A (2010) Enhanced adsorption of methylene blue from aqueous solution by chitosan-g-poly (acrylic acid)/vermiculite hydrogel composites. J Environ Sci 22:486–493

18. Rafatullah M, Sulaiman O, Hashim R, Ahmad A (2010) Adsorption of methylene blue on low-cost adsorbents: a review. J Hazard Mater 177:70–80

19. Ahmed EM, Aggor FS, Awad AM, EI-Aref AT (2013) An innovative method for preparation of nanometal hydroxide superabsorbent hydrogel. Carbohydr Polym 91:693–698

20. Caló E, Khutoryanskiy VV (2015) Biomedical applications of hydrogels: a review of patents and commercial products. Eur Polym J 65:252

21. Ahmed EM (2015) Hydrogel: preparation, characterization, and applications: a review. J Adv Res 6:105

22. Krušić MK, Milosavljević N, Debeljković A, Üzüm OB, Karadağ E (2012) Removal of Pb2+ions from water by poly(acrylamide-co-sodium methacrylate) hydrogels. W Air Soil Pollut 223:4355–4368

23. Barakata MA, Sahiner N (2008) Cationic hydrogels for toxic arsenate removal from aqueous environment. J Environ Manag 88:955–961

24. Vivek AV, Dhamodharan R (2008) Amphiphilic polystyrene-graft-poly (N, N-dimethylamino-2-ethyl methacrylate) hydrogels synthesized via room temperature ATRP: studies on swelling behaviour and dye sorption. React Funct Polym 68:967–973

25. Reena S, Balbir SK, Susheel K, Pathania D, Amit K, Neha S, Reva MS, Caroline S (2015) Biodegradable and conducting hydrogels based on guar gum polysaccharide for antibacterial and dye removal applications. J Environ Manag 162:37–45

26. Kashma S, Balbir SK, Vijay K, Vinod K, Sudipta S, Susheel K, Hendrik CS (2013) Synthesis and properties of poly(acrylamide-aniline)-grafted gum ghatti based nanospikes. RSC Adv 3:5830–25839

27. Mittal H, Maity A, Ray SS (2016) Gum karaya based hydrogel nanocomposites for the effective removal of cationic dyes from aqueous solutions. Appl Surf Sci 364:917–930

28. Amit KS, Priya Balbir SK, Sagar P, Jaspreet KB, Sakshi B, Vaishali T, Nisha S (2019) Response surface methodology directed synthesis of luminescent nanocomposite hydrogel for trapping anionic dyes. J Environ Manag 231:380–390

29. Bhatnagar A, Sillanpää M (2009) Applications of chitin- and chitosan-derivatives for the detoxification of water and wastewater-a short review. Adv Colloid Interface Sci 152(1–2):26–38

30. Gholam RM, Fatemeh B, Behnam S (2015) Kappa-carrageenan beads as new adsorbent to remove crystal violet dye from water: adsorption kinetics and isotherm. Desalination Water Treat 53:2529–2539

31. Ekici S, Isıkver Y, Saraydın D (2006) Poly(acrylamide–sepiolite) composite hydrogels: preparation, swelling and dye adsorption properties. Polym Bull 57:231–241

32. Oladipo AA, Gazi M, Saber-Samandari S (2014) Adsorption of anthraquinone dye onto eco-friendly semi-IPN biocomposite hydrogel: equilibrium isotherms, kinetic studies and optimization. J Taiwan Inst Chem Eng 45:653–664

33. Abdel-Halim ES (2013) Preparation of starch/poly (N, N-diethylaminoethyl methacrylate) hydrogel and its use in dye removal from aqueous solutions. React Funct Polym 73:1531–1536

34. Şolpan D, Şen M, Kölge Z (2008) Güven O adsorption of apollo reactive dyes on poly(N, N dimethylamino ethylmethacrylate) hydrogels. Radiat Phys Chem 77:428–433

35. Ho YS, McKay G (1999) The sorption of lead(II) ions on peat. Water Res 33:578–584

36. Kaith BS, Jindal R, Mittal H, Kumar K (2012) Synthesis, characterization, and swelling behavior evaluation of hydrogels based on Gum ghatti and acrylamide for selective absorption of saline from different petroleum fraction–saline emulsions. J Appl Polym Sci 124:2037–2047

37. Makhado E, Pandey S, Nomngongo PN, Ramontja J (2018) Preparation and characterization of xanthan gum-cl-poly(acrylic acid)/o-MWCNTs hydrogel nanocomposite as highly effective reusable adsorbent for removal of methylene blue from aqueous solutions. J Colloid Interface Sci 513:700–714

38. Soleimani K, Tehrani AD, Adeli M (2018) Preparation of new GO-based slide ring hydrogel through a convenient one-pot approach as methylene blue absorbent. Carbohydr Polym 187:94–101

39. Dai H, Huang H (2016) Modified pineapple peel cellulose hydrogels embedded with sepia ink for effective removal of methylene blue. Carbohydr Polym 148:1–10

40. Betül T, Deniz IC, Süreyya M (2017) Preparation of N-isopropylacrylamide/itaconic acid/pumice highly swollen composite hydrogels to explore their removal capacity of methylene blue. Colloids Surf A Physicochem Eng Asp 519:245–253

41. Reena S, Susheel K, Balbir S, Deepak P, Amit K, Pankaj T (2015) Guaran-based biodegradable and conducting interpenetrating polymer network composite hydrogels for adsorptive removal of methylene blue dye. Polym Degrad Stab 122:52–65

42. Chengmei S, Furong T, Yuezhi C (2018) Evaluation of nitriloacetic acid modified cellulose film on adsorption of methylene blue. Int J Biolo Macromol 114:400–407

43. Sharma K, Kumar V, Kaith BS, Kumar V, Som S, Pandey A, Kalia S, Swart HC (2015) Evaluation of a conducting interpenetrating network based on gum ghatti-g-poly(acrylicacid-aniline) as a colon-specific delivery system for amoxicillin trihydrate and paracetamol. New J Chem 39:3021–3034

44. Karthika JS, Vishalakshi B (2015) Novel stimuli - responsive gellan gum - graft - poly(DMAEMA) hydrogel as adsorbent for anionic dye. Int J Biolo Macromol 81:648–655

45. Krishna KA, Vishalakshi B (2017) Gellan gum-based novel composite hydrogel: evaluation as adsorbent for cationic dyes. J Appl Polym Sci 134:45527

46. Fosso-Kankeu E, Mittal H, Mishra SB, Mishra AK (2015) Gum ghatti and acrylic acid based biodegradable hydrogels for the effective adsorption of cationic dyes. J Ind Eng Chem 22:171–178

47. Gan L, Shang SM, Hu EL, Wah C, Yuen M, Jiang SX (2015) Konjac glucomannan/graphene oxide hydrogel with enhanced dyes adsorption capability for methyl blue and methyl orange. Appl Surf Sci 357:866–872

48. Ramasubramaniam S, Govindarajan C, Nasreen K, Sudha PN (2014) Removal of cadmium (II) ions from aqueous solution using chitosan/starch polymer blend. Comput Interface 21:95–109

49. Alencar WS, Acayanka E, Lima EC, Royer B, de Souza FE, Lameira J, Alves CN (2012) Application of Mangifera indica (mango) seeds as a biosorbent for removal of Victazol Orange 3R dye from aqueous solution and study of the biosorption mechanism. Chem Eng J 209:577–588

50. Melo BC, Paulino FAA, Cardoso VA, Pereira AGB, Fajardo AR, Rodrigues FHA (2018) Cellulose nanowhiskers improve the methylene blue adsorption capacity of chitosan-g poly(acrylic acid) hydrogel. Carbohydr Polym 181:358–367

51. Lessa EF, Gularte MS, Garcia ES, Fajardo AR (2017) Orange waste: a valuable carbohydrate source for the development of beads with enhanced adsorption properties for cationic dyes. Carbohydr Polym 157:660–668

52. Liu Y, Zheng YA, Wang AQ (2011) Effect of biotite content of hydrogels on enhanced removal of methylene blue from aqueous solution. Ionics 17:535–543

53. Hosseinzadeh H, Ramin S (2018) Fabrication of starch-graft-poly (acrylamide)/graphene oxide/hydroxyapatite nanocomposite hydrogel adsorbent for removal of malachite green dye from aqueous solution. Int J Biolo Macromol 106:101–115

54. Weber WJ, Morris JC (1963) Kinetics of adsorption on carbon solution. J Sanit Eng Div Eng 89:31–60

55. Crini G, Peindy HN, Gimbert F, Robert C (2007) Removal of C.I. Basic green 4 (malachite green) from aqueous solutions by adsorption using cyclodextrin-based adsorbent: kinetic and equilibrium studies. Sep Purif Technol 53:97–110

56. Hameed BH, Tan IAW, Ahmad AL (2008) Adsorption isotherm, kinetic modeling and mechanism of 2,4,6-trichlorophenol on coconut husk-based activated carbon. Chem Eng J 144:235–244